



ISSN: 2447-3359

REVISTA DE GEOCIÊNCIAS DO NORDESTE

*Northeast Geosciences Journal*

v. 7, nº 2 (2021)

<https://doi.org/10.21680/2447-3359.2021v7n2ID20423>



## ESTIMATING INVASIVE GRASSES HEIGHTS WITH IMAGES FROM A UNMANNED AERIAL VEHICLE IN BRAZILIAN CERRADO: ACCURACY OF GLOBAL NAVIGATION SATELLITE SYSTEM FROM PHANTOM 4

**Dhonatan Diego Pessi<sup>1</sup>; Jefferson Vieira José<sup>2</sup>;  
Camila Leonardo Miotto<sup>3</sup>; Marco Antonio  
Diodato<sup>4</sup>; Alfredo Marcelo Grigio<sup>5</sup>; Antonio  
Conceição Paranhos Filho<sup>6</sup>; Normandes Matos da  
Silva<sup>7</sup>**

<sup>1</sup>PhD Student in Environmental Technologies, Postgraduate Program in Environmental Technologies, Federal University of Mato Grosso do Sul (UFMS), Campo Grande/MS, Brasil.

**ORCID:** <https://orcid.org/0000-0003-0781-785X>

Email: dhonatan.pessi@gmail.com

<sup>2</sup>PhD in Science with area of expertise in Agricultural Systems Engineering from ESALQ/USP, Adjunct Professor-A in the Irrigation, Hydrology and Drainage, Hydraulics and Rural Constructions area of the Agronomy and Forest Engineering course, Federal University of Acre, Cruzeiro do Sul/AC, Brasil.

**ORCID:** <https://orcid.org/0000-0003-1384-0888>

Email: jfvieira@usp.br

<sup>3</sup>PhD in Environmental Sanitation and Water Resources at UFMS, Adjunct Professor A2 at the Institute of Agrarian and Technological Sciences (ICAT), Federal University of Rondonópolis (UFR), Rondonópolis/MS, Brasil.

**ORCID:** <https://orcid.org/0000-0002-6951-9527>

Email: ea.miotto@gmail.com

<sup>4</sup>PhD in Biological Sciences from the Federal University of Paraná. Associate professor at the Federal University Rural do Semi-Árido-UFERSA, Mossoró/RN, Brasil.

**ORCID:** <https://orcid.org/0000-0002-9088-836X>

Email: diodato@ufersa.edu.br

<sup>5</sup>PhD in Geodynamics from the Federal University of Rio Grande do Norte. Adjunct Professor II at the State University of Rio Grande do Norte, Mossoró/RN, Brasil.

**ORCID:** <https://orcid.org/0000-0002-2094-9710>

Email: alfredogrigio1970@gmail.com

<sup>6</sup>Lecturer Degree in Institute of Geosciences at USP, Titular Professor at the Faculty of Engineering, Architecture and Urbanism and Geography (FAENG), Federal University of Mato Grosso do Sul (UFMS), Campo Grande/MS, Brasil.

**ORCID:** <https://orcid.org/0000-0002-9838-5337>

Email: antonio.paranhos@ufms.br

<sup>7</sup>PhD in Ecology of Terrestrial and Aquatic Ecosystems at USP, Associate Professor at the Institute of Agrarian and Technological Sciences (ICAT), Federal University of Rondonópolis, (UFR), Rondonópolis/MT, Brasil.

**ORCID:** <https://orcid.org/0000-0002-4631-9725>

Email: normandes@ufr.edu.br

### Abstract

The purpose of this study was to estimate the height of invasive plants from UAV images using the GNSS integrated into the UAV and to evaluate the accuracy of the GNSS(I) (integrated in UAV) relative to Topcon's GNSS(RTK). DSM and DTM elevation models were produced from images collected by unmanned aerial vehicle. The production of CHIS occurred through the subtraction of the DSM and the DTM. In order to assess the accuracy of the CHIS+GNSS(I) model, the CHIS+GNSS(RTK) model was generated as the observed variable. The comparison between the models took place in two sample areas represented by typical vegetation of Cerrado and Brachiaria grass. The statistical tests adopted were: Spearman correlation, RMSE, MAE and Wilcoxon test. The visual interpretation of the selected images showed that the CHIS+GNSS(I) model presented errors in the identification of the ground cover represented by invasive grasses when compared to the CHIS+GNSS(RTK) model, being less accurate in the classification of the canopy heights of the invasive species. Statistical tests indicated that the CHIS+GNSS(I) model showed significant differences in the identification of invasive species, with greater height error (0.24 cm) in the sample area. From these results it can be seen that the CHIS+GNSS(RTK) model is more assertive in detecting ground cover composed by exotic grasses than the CHIS+GNSS(I) model.

**Keywords:** Drones; Environmental management; Invasive plants; Remote sensing; Precision agriculture.

#### **ESTIMANDO A ALTURA DE GRAMÍNEAS INVASORAS COM IMAGENS DE UM VEÍCULO AÉREO NÃO TRIPULADO NO CERRADO BRASILEIRO: PRECISÃO DO SISTEMA GLOBAL DE NAVEGAÇÃO POR SATÉLITE DO PHANTOM 4**

##### **Resumo**

O objetivo deste estudo foi estimar a altura de plantas invasoras a partir de imagens de veículo aéreo não tripulado (VANT) usando o GNSS integrado ao VANT e avaliar a precisão do GNSS(I) (integrado ao VANT) em relação ao GNSS(RTK) Topcon. Modelos de elevação DSM e DTM foram produzidos a partir de imagens coletadas por veículos aéreos não tripulados. A produção de CHIS ocorreu por meio da subtração do DSM e do DTM. Para avaliar a precisão do modelo CHIS+GNSS(I), o modelo CHIS+GNSS(RTK) foi gerado como a variável observada. A comparação entre os modelos ocorreu em duas áreas amostrais representadas por vegetação típica de Cerrado e capim-braquiária. Os testes estatísticos adotados foram: correlação de Spearman, RMSE, MAE e teste de Wilcoxon. A interpretação visual das imagens selecionadas mostrou que o modelo CHIS+GNSS(I) apresentou erros na identificação da cobertura do solo representada por gramíneas invasoras quando comparado ao modelo CHIS+GNSS(RTK), sendo menos preciso na classificação das alturas do dossel das espécies invasoras. Testes estatísticos indicaram que o modelo CHIS+GNSS(I) apresentou diferenças significativas na identificação de espécies invasoras, com maior erro de altura (0,24 cm) na área amostrada. A partir desses resultados, pode-se verificar que o modelo CHIS+GNSS(RTK) é mais assertivo na detecção de cobertura do solo composta por gramíneas exóticas do que o modelo CHIS+GNSS(I).

**Palavras-chave:** Drones; Gestão ambiental; Plantas invasoras; Sensoriamento remoto, Agricultura de precisão.

#### **ESTIMACIÓN DE ALTURAS DE PASTOS INVASORES CON IMÁGENES DE UN VEHÍCULO AÉREO NO TRIPULADO EN EL CERRADO BRASILEÑO: PRECISIÓN DEL SISTEMA DE NAVEGACIÓN POR SATÉLITE GLOBAL DEL PHANTOM 4**

##### **Resumen**

El propósito de este estudio fue estimar la altura de plantas invasoras a partir de imágenes de UAV utilizando el GNSS integrado en el UAV y evaluar la precisión del GNSS(I) (integrado en el UAV) en relación a GNSS(RTK) Topcon. Los modelos de elevación DSM y DTM se elaboraron a partir de imágenes recopiladas por vehículos aéreos no tripulados. La producción de CHIS se consiguió mediante la sustracción del DSM y del DTM. Para evaluar la precisión del modelo CHIS+GNSS(I), se generó el modelo CHIS+GNSS(RTK) como variable observada. La comparación entre los modelos se realizó en dos áreas de muestreo con vegetación típica de pasto Cerrado y Brachiaria. Las pruebas estadísticas adoptadas fueron: correlación de Spearman, RMSE, MAE y prueba de Wilcoxon. La interpretación visual de las imágenes seleccionadas mostró

que el modelo CHIS+GNSS(I) presentó errores en la identificación de la cobertura vegetal representada por pastos invasores cuando se comparó con el modelo CHIS+GNSS(RTK), siendo menos preciso en la clasificación de las alturas del dosel de las especies invasoras. Las pruebas estadísticas indicaron que el modelo CHIS+GNSS(I) mostró diferencias significativas en la identificación de especies invasoras, con mayor error de altura (0,24 cm) en el área de muestreo. A partir de estos resultados, se puede ver que el modelo CHIS+GNSS(RTK) es más assertivo en la detección de la cobertura del suelo compuesta por pastos exóticos que el modelo CHIS+GNSS(I).

**Palabras-clave:** Drones; Gestión ambiental; Plantas invasoras; Teledetección, Agricultura de precisión.

#### **1. INTRODUCTION**

Protected areas are natural spaces of high ecological value that aim at safeguarding biodiversity, preserving ecosystem services and ensuring the integrity of the natural heritage. The conservation of these ecosystems requires environmental monitoring procedures. However, obtaining financial resources to deal with a growing variety of activities related to the management of their environmental resources is generally insufficient (WATSON *et al.*, 2014), seriously affecting the effectiveness of the final results of projects (JUFFE-BIGNOLI *et al.*, 2014).

Protected areas subject to international and national agreements must deal with their acquired responsibilities in order to maintain their legal status (GONÇALVES *et al.*, 2016), i.e., the conservation projects of these spaces must be effective and perennial. There is a demand for cost-effective, versatile and practical initiatives to fulfill many requirements to ensure conservation, including a wide range of solutions (LOPOUKHINE *et al.*, 2012), technological advances and innovative methods or applications of existing technologies (LÓPEZ; MULERO-PAZMÁNY, 2019).

Over the last decade, the Unmanned Aerial Vehicle (UAV), also popularly known as drones, have been the subject of growing interest in the civil and scientific realm, being considered a disruptive technology within remote sensing (MELESSE *et al.*, 2007; LÓPEZ; MULERO-PÁZMÁNY, 2019), including for environmental studies (WHITEHEAD; HUGENHOLTZ, 2014).

Drones represent a strategy with relatively low risk of accidents and low financial cost to quickly and systematically observe natural phenomena in high spatiotemporal resolution (RODRÍGUEZ *et al.*, 2012; LÓPEZ; MULERO-PÁZMÁNY, 2019). For these reasons, drones have recently become a major trend in wildlife research (LINCHANT *et al.*, 2015; CHRISTIE *et al.*, 2016) and environmental management (MULERO-PÁZMÁNY *et al.*, 2014; CHABO; BIRD, 2015).

Given the wide range of possibilities, it is not surprising that some protected areas are adopting drones for various applications. For example, for monitoring invasive plant species (MICHEZ *et al.*, 2016; DVORÁK *et al.*, 2015; HUNG *et al.*, 2014; WAN *et al.*, 2014; KNOTH *et al.*, 2013; PEÑA *et al.*, 2013; ZAMAN *et al.*, 2011); for documenting illegal logging and mining (KOH; WICH, 2012); in the classification methods using canopy height (MATESE *et al.*, 2017; STROPPIANA *et al.*, 2018; ZILIANI *et*

al., 2018; VILJANEN *et al.*, 2018; DE SÁ *et al.*, 2018; MARTIN *et al.*, 2018), including for identifying species of interest through suborbital images. Recently, a team of scientists discovered a biodiversity hotspot using drones (LÓPEZ; MULERO-PÁZMÁNY, 2019), which could be discussed as a convenient procedure to properly expand protected areas, as established by Aichi Target 11 (JUFFE-BIGNOLI *et al.*, 2014).

We are witnessing a continuous development of sophisticated drones and inventive methods that target specific conservation actions, such as fighting forest fires (KRULL *et al.*, 2012; MERINO *et al.*, 2012; ZHANG *et al.*, 2015) and planting seeds for reforestation (FORTES, 2017). The rapid pace of technological advances and new applications has probably exceeded previous expectations, but it also gives rise to unique circumstances that must be placed in the context of management (LÓPEZ; MULERO-PÁZMÁNY, 2019).

The objective of this research was to estimate the height of invasive plants from UAV images using the GNSS integrated into the UAV (GNSS(I)) and to evaluate the accuracy of the GNSS

from the correction of the image mosaic carried out with a global positioning system with centimeter accuracy (GNSS(RTK)), corrected with dots controls obtained by RTK (Real-time Kinematic).

## 2. METODOLOGY

### 2.1. Description of the study area

The study area is located at the Universidade Federal de Rondonópolis (Figure 1), in Rondonópolis, Mato Grosso, Brazil. The study area presents elements of remaining vegetation of Cerrado stricto sensu, exposed soil sections and environments with exotic and invasive species, predominantly *Urochloa* ssp. The study area covered three hectares. Local climate characteristic is defined as CWA (humid subtropical climate) with annual average rainfall of 1500 mm and temperature of 25°C, Table 1 (SOUZA *et al.*, 2013; PEEL *et al.*, 2007).

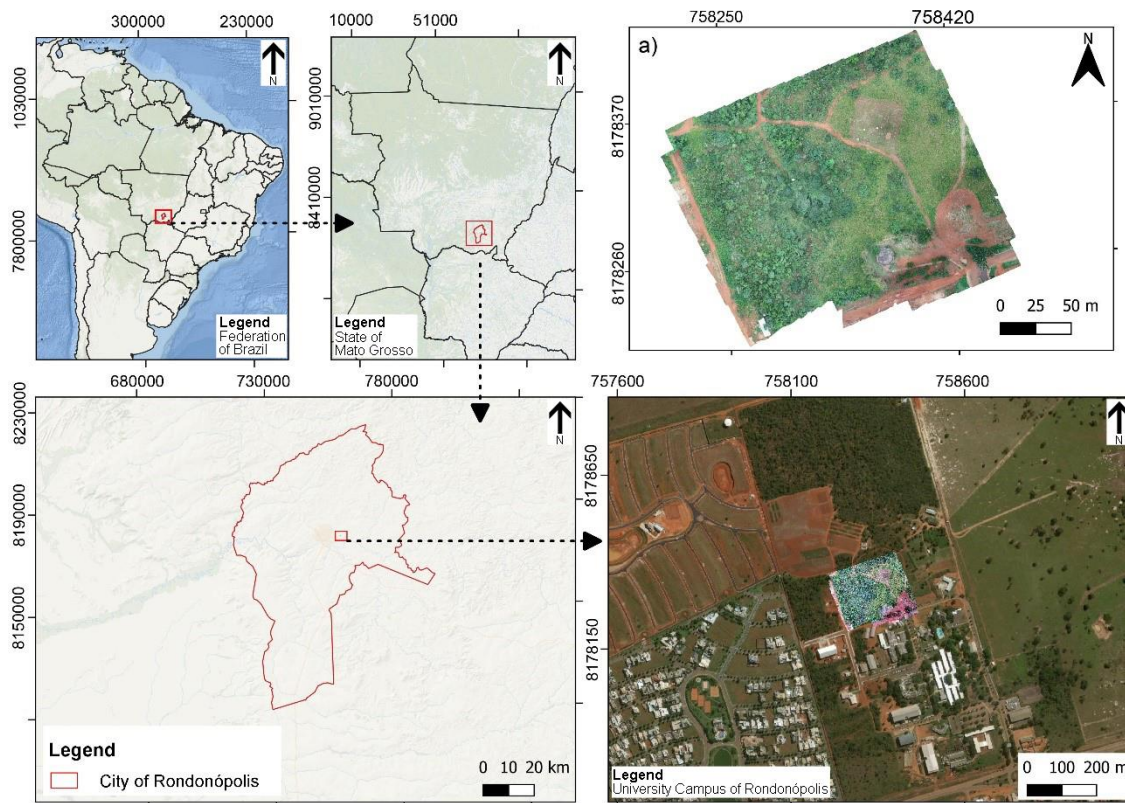


Figure 1 - General location of the study area. In a) experimental site with the orthomosaic images obtained by UAV. UTM Coordinate System, SIRGAS 2000, 21S. Source: Vector data, IBGE (2019); satellite imagery, Google (2019); orthomosaic image, The authors.

The soil class characteristics, climate, temperature and mean annual precipitation, longitude and latitude, biome and altitude of the study area are presented in Table 1.

Table 1 - Data on latitude, longitude, soil type, annual average temperature and rainfall, climate and altitude of the study area. Source: Temperature and rainfall data (SOUZA *et al.*, 2013); climate data (PEEL *et al.*, 2007); soil data (EMBRAPA, 2006). Caption: CWA (Humid Subtropical Climate). Source: The authors.

Biome	Altitude	Latitude	Longitude	Climate	Soil Type	Annual Average	
						Rainfall	Temperature
Cerrado	293 m	16°27'40"	54°34'52"	Cwa	Dystrophic Red Latosol	1500 mm	25°C

## 2.2. Field data acquisition

In order to acquire the images, it was carried out the flight plan executed by the DroneDeploy platform, available at: <https://support.dronedeploy.com/lang-en-BR>, on February 2, 2019, using the UAV Phantom 4 Pro from DJI fitted with a regular RGB camera, 20 megapixel (MP) sensor.

It was necessary to collect control points manually in the field with the height information of the invasive species observed in the study area (*Urochloa ssp*) in order to use them in the comparison of the data estimated by the CHIS+GNSS(I) model (canopy height invasive species). The points were collected using a GNSS (GPS receiver, Garmin 76CSx, Olathe, KS, USA). In total, 18 field reference points were collected, associated with height measurements of invasive species, measured with a tape measure.

## 2.3. Control point collection by RTK

Seven ground control points (GCPs) were collected. These points were embodied by 0.4 m square white plastic plates placed in the study area to ensure the positional accuracy of the central coordinates of photography obtained by the drone geolocation system. Usually these coordinates are subjected to positional errors that can vary from five to ten meters, on the X (longitude), Y (latitude) and Z (altitude) axes. The GCPs were georeferenced with a Topcon Hiper V RTK system, which has an average precision on the XYZ axes of  $\pm 0.005$  m. In the photo mosaic elaboration step, GCPs were used to adjust the positioning error of the images, using the PPK (Post Processed Kinematic) positional accuracy postprocessing technique. The landmarks (GCPs) were inserted in the images manually in Agisoft Photoscan Professional software (version 1.4.0, Agisoft, St. Petersburg, Russia).

## 2.4. Data processing

### 2.4.1. Images

All UAV data was preprocessed and delivered using Structure from Motion (SfM) available at Agisoft Photoscan. In addition to providing the orthophotographs of the study area with 3-band (RGB), the SfM by-products of the Digital Surface Model (DSM) and Digital Terrain Model (DTM) were also elaborated. DTM was obtained through semi-supervised densified point cloud classification methods. The canopy height model (CHM) was obtained by subtracting the MDT and MDS from by using the R software (R CORE TEAM, 2019) with the raster package (HIJMANS, 2017).

### 2.4.2. Invasive species CHIS+GNSS(I)

In order to calculate the canopy height model of the invasive species it was necessary to select in the CHM model the height established for the invasive species, by doing so the minimum value of 49 cm and maximum value of 110 cm for *Urochloa ssp.* were established according to data collected in the field. However, it was decided to set different values from those observed in the field, plus and minus, in order to consider the possible differences in the model (errors). Thus, the program was informed to select values ranging from 20 cm to 140 cm. The procedures were performed in the software R (R CORE TEAM, 2019) with the following packages: (i) data processing raster package (HIJMANS, 2017), *rgdal* (BIVAND, 2018); (ii) plotting the results lattice package (DEEPAYAN, 2008), *rasterVis* (LAMIGUEIRO; HIJMANS, 2018), *gridExtra* (AUGUIE, 2017), *RColorBrewer* (NEUWIRTH, 2014).

## 2.5. Validation

### 2.5.1. Visual comparison of results

It was decided to compare the results from two sample areas (Figure 2), only places where there is invasive plants and remaining vegetation confirmed in the fieldwork.

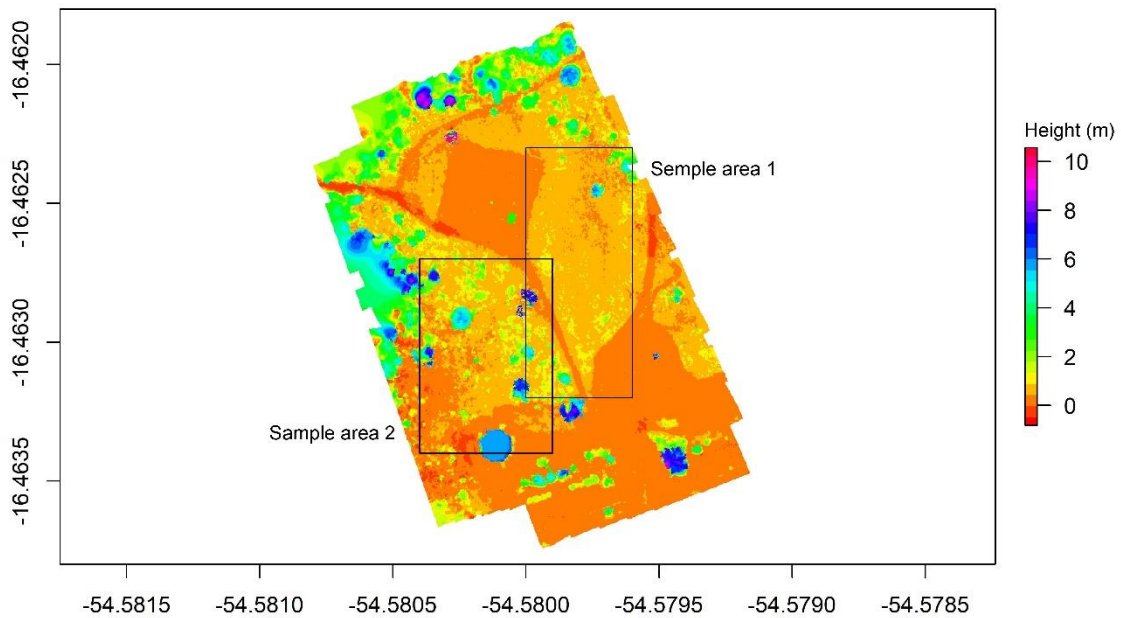


Figure 2 - Location of sample areas used to compare the results of both models (CHIS+GNSS(I) and CHIS+GNSS(RTK)). Source: The authors.

### 2.5.2. Statistical analysis

In order to validate the accuracy of the CHIS+GNSS(I) (estimated variable) in identifying invasive species, it was compared with the CHIS+GNSS(RTK) (observed variable), therefore, it was necessary to select 1000 sample points from each area from a pixel grid (Figure 3) generated using the R. software,

in which it is informed the amount of numbers to be collected in a given raster, and each grid point represents an average of the pixel values corresponding to he analyzed raster. The values of the averages of the collected points were released in a data frame file and later it was performed the deletion of the points where there was absence of information Figure 3.

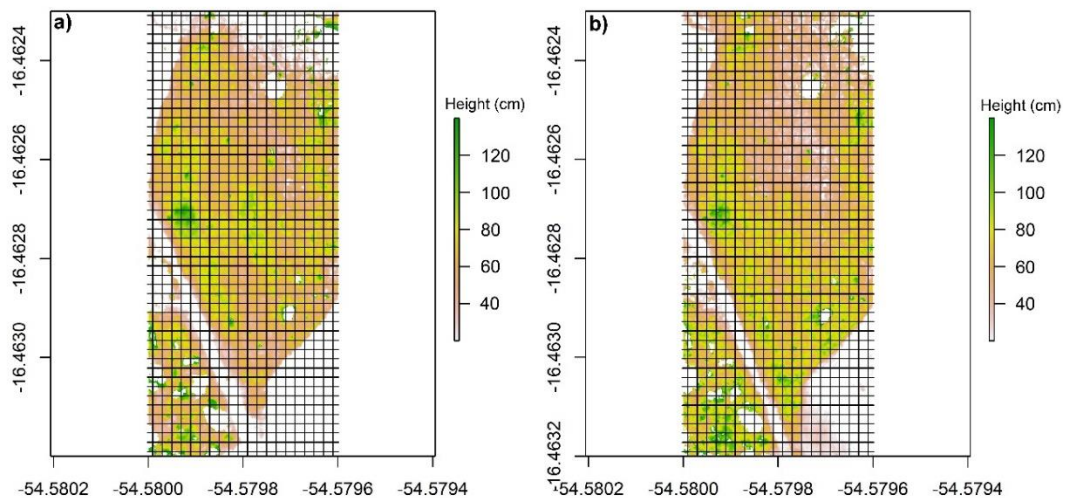


Figure 3 - Example of grid generated to collect 1000 sampling points. Each grid square corresponds to one sample point. In (a) sample area 1 with CHIS+GNSS(I) and in (b) sample area 1 with CHIS+GNSS(RTK). Source: The authors.

In the statistical analysis, the tests of Spearman correlation coefficients (SCC), root-mean-square error (RMSEZ) of the canopy height, mean absolute error (MAEZ) of the canopy height and Wilcoxon test were performed. All values used as a variable observed in the accuracy analysis of the GNSS(I) model were used from the values extracted from the GNSS(RTK) model.

Spearman's correlation coefficient is a nonparametric classification test (distribution-free) proposed as a measure of the strength of the association between two variables. It is a measure of a monotonous association that is used when data distribution makes Pearson's correlation coefficient undesirable or misleading (HAUKE; KOSSOWSKI, 2011).

The relationship (or correlation) between the two variables is denoted by the letter *r* and is quantified with a number ranging from -1 to +1. Zero means no correlation, with 1 (one) meaning a complete or perfect correlation Table 2.

Table 2 - Interpretation of Spearman correlation coefficients according to Akoglu (2018) and Fowler (2009). Source: The authors.

Correlation Coefficient		Correlation Strength
+ 1	- 1	Perfect
+ 0,70 a + 0,90	- 0,70 a - 0,90	Strong
+ 0,40 a + 0,60	- 0,40 a - 0,60	Moderate
+ 0,10 a + 0,30	- 0,10 a - 0,30	Weak
0	0	None

RMSE has been used as a statistical metric to measure model performance in meteorology, air quality and climate studies. MAE is another useful measurement widely used in model evaluations. Although both have been used to evaluate model performance for many years, there is no consensus on the most appropriate metric for model errors. In the field of geosciences,

many present RMSE as a standard metric for model errors (MCKEEN *et al.*, 2005; SAVAGE *et al.*, 2013; CHAI *et al.*, 2013), while others choose to avoid RMSE and present only the MAE (CHAI; DRAXLER, 2014). In this study we have chosen both tests as metric measure to provide error data in the distribution of the assigned values.

The Wilcoxon test is a nonparametric statistical hypothesis used to compare two related samples, paired samples, or repeated measurements in a single sample in order to assess whether their mean population ratings differ. It can be used as an alternative to the paired student t-test, combined paired t-test or dependent sample t-test when the population cannot be regarded as being normally distributed. It is a nonparametric test that can be used to determine if two dependent samples were selected from populations with the same distribution (KLOBE; MCKEAN, 2014).

### 3. RESULTS

#### 3.1. Evaluation of the CHIS+GNSS(I) model accuracy in comparison with CHIS+GNSS(RTK) model

Visual observation of the image mosaic allows us to identify differences between the two models, especially when comparing the lower left side and the upper part of the figures. In general, it is noticed that there was a difference in the spatialization and interpretation of the heights of invasive species in the analyzed models.

Through a visual interpretation it can be seen differences related to height, comparing Figures 4a and 4b, mainly in the lower left side of the Figure 4a and the upper part of the Figure 4a. It can be seen in the Figure 4b (CHIS+RTK) that there was a difference in the spatialization and interpretation of the heights of invasive species compared to Figure 4a.

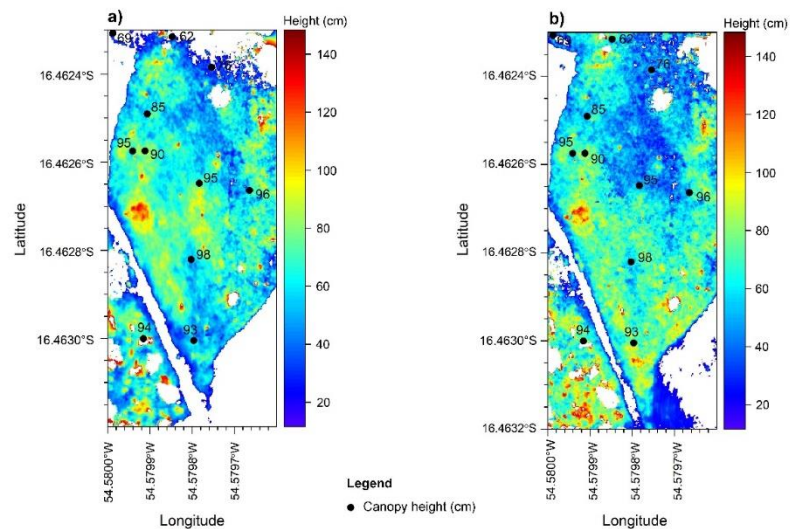


Figure 4 - Comparison between CHIS+GNSS(I) (a) and CHIS+GNSS(RTK) (b) models in sample area 1. Source: The authors.

The regions shown in Figure 5 were the places where the most pronounced visual differences occurred in the canopy heights of the invasive species, and in some places there was also lack of

information (probably values below 20 cm) in the CHIS+GNSS(I) model (Figure 5a and Figure 5c) compared to the CHIS+GNSS(RTK) model (Figure 5b and Figure 5d).

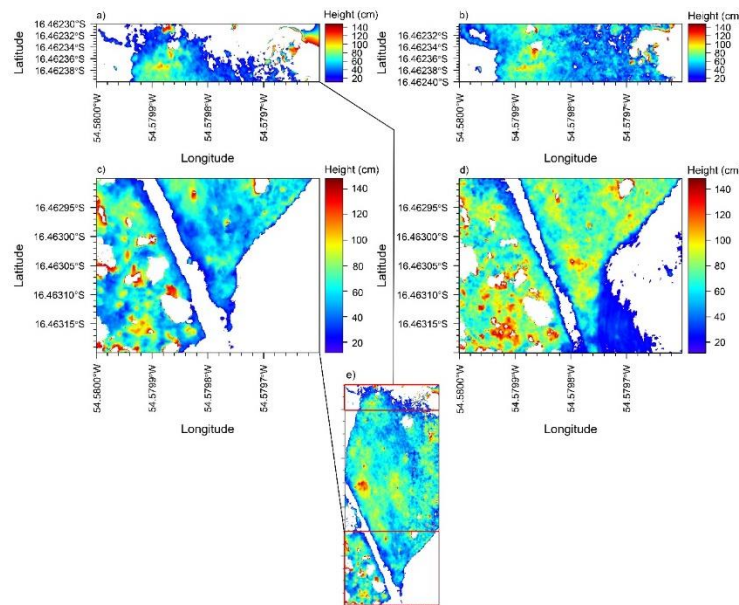


Figure 5 - (a) and (b) a cutout of the upper part of (e); (c) and (d) a cutout from the bottom of (e); (a) and (c) represents the CHIS+GNSS(I) model and (b) and (d) represents the CHIS+GNSS(RTK) model. Source: The authors.

In this region there were flaws in the model for proper identification of invasive species when compared to Figure 5b (CHIS+GNSS(RTK)). This lack of information may be related to the accuracy of the CHIS+GNSS(RTK) model, since the height recorded in this region was very low (between 20 cm and 40 cm), being required more precision to identify smaller vegetation.

In Figure 5c there was a higher heterogeneity in heights compared to Figure 5d, in which heights are more homogeneous. In the left part of Figure 5c there are low values (20 cm to 40 cm), and this height scale was only present in the edges (corridor

between the two vegetation fragments) and in the lower right side (herbaceous region) of Figure 5d.

The CHIS+GNSS(RTK) model was more sensitive in identifying small species (up to 40 cm) when compared to the evaluated model (CHIS+GNSS(I)). The use of the CHIS+GNSS(RTK) model is essential as a product for decision making in agricultural management, when it is necessary to evaluate areas with presence of graminoid size invasive plants, known in the agricultural area as weeds, which are generally small. With the CHIS+GNSS(I) model this might not be possible, as height errors are more variable.

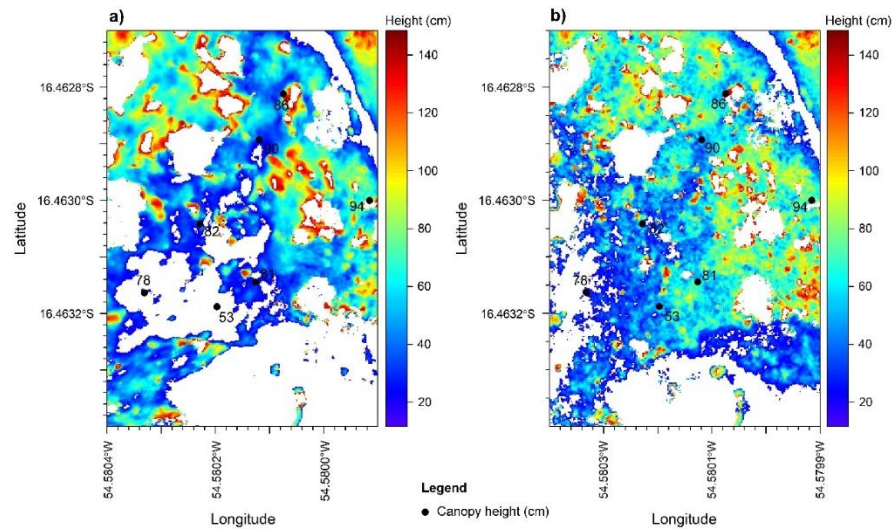


Figure 6 - Comparison between CHIS+GNSS(I) (a) and CHIS+GNSS(RTK) (b) models in sample area 2. Source: The authors.

As in sample area 1, it can be seen in Figure 6a differences in model classification, that is, absence of canopy height information of invasive species in some regions of the figure when compared to Figure 6b. In Figure 6b the distribution of heights is more consistent with the information gathered in the field, as can be seen from the control points in the figures.

Figure 7 illustrates the area in which a large difference in canopy height of invasive species occurred. As shown in Figure

7a, there is a lack of height information in a region where values are very low (20 cm to 30 cm) in comparison with Figure 7b. As these are very low values, it is expected that inaccuracy will occur from the CHIS+GNSS(I) model. In addition to the absence, it can also be analyzed that canopy height values are not similar to Figure 7b, where heights are better distributed and more consistent with field data (Figure 7b).

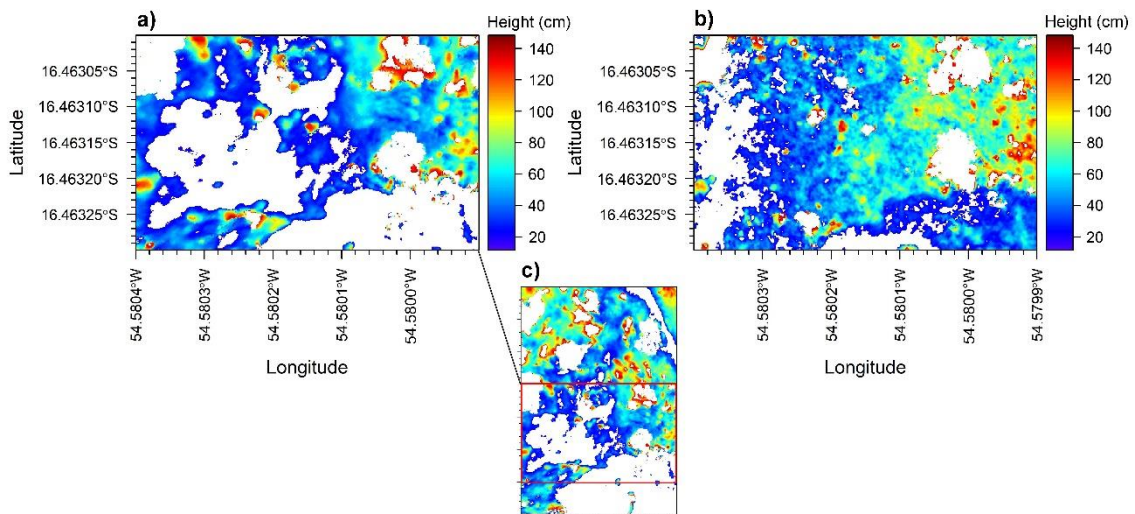


Figure 7 - In (a) and (b) a cutout of the central lower part of Figure 7 (c); (a) represents the CHIS+GNSS(I) model and (b) represents the CHIS+GNSS(RTK) model. Source: The authors.



### 3.2. Statistical analysis results

The Spearman correlation classification between the estimated model (CHIS+GNSS(I)) and the observed model

(CHIS+GNSS(RTK)) for the two sample areas is presented in Figure 8.

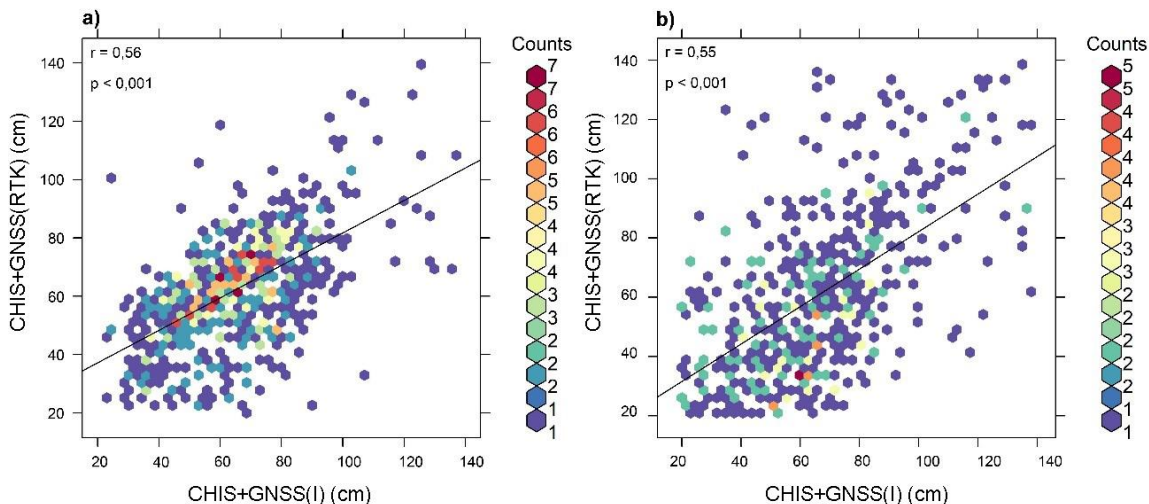


Figure 8 - Spearman correlation between the CHIS+GNSS(I) and CHIS+GNSS(RTK) models. In (a) sample area 1 and in (b) sample area 2. In (a) 684 points were analyzed and in (b) 506 points were analyzed. The difference in points between the two areas is due to the lack of information (NA) in some places in the area. Sample area 2 showed more clearly the difference between the two models (Figure 6). Source: The authors.

The data show a significant and median correlation strength for sample area 1 ( $r = 0.56$ ,  $p < 0.001$ ) and for sample area 2 ( $r = 0.55$ ,  $p < 0.001$ ). The correlation was significant but moderate. This is due to the accuracy of the canopy measurement process from calibration using RTK (CHIS+GNSS(RTK) model). This

model is the most accurate on all spatial axes with low margin of error. Measurement data from the UAV GNSS were calculated with greater inaccuracy across all spatial axes (Table 3) when calculating the dense point cloud in PhotoScan, which may explain some differences in the compared models.

Table 3 - Spatial axes error from GNSS(I) data and GNSS(RTK) data. Source: Error report generated in Agisoft PhotoScan 1.4.0 software.

Equipment	Error X (cm)	Error Y (cm)	Error Z (cm)	Error XY (cm)	Total Error (cm)
GNSS	169	79	75	186	201
RTK	4,86	4,82	0,57	6,85	6,87

The nonparametric statistical error tests in the evaluated model (MAEZ and RMSEZ) and the Wilcoxon test for both sample areas are shown in Table 4.

Table 4 - Statistical tests between the estimated variable (CHIS+GNSS(I)) and the observed variable (CHIS+GNSS(RTK)). Source: The authors.

Sample area	RMSE <sub>Z</sub> (cm)	MAE <sub>Z</sub> (cm)	Wilcoxon
1	0,17	0,12	0,0117
2	0,24	0,19	$p < 0,001$

Sample area 1 was the one with the lowest error metric, with 0.12 cm error for MAEZ, and 0.17 cm error for RMSEZ, while

sample area 2 had the largest error, ranging from 0.19 cm for MAEZ to 0.24 for RMSEZ. UAV estimations from GNSS(I) showed greater errors in canopy altitude accuracy of invasive species in sample area 2.

Considering the two sample areas, the results of the test of significant difference between related samples were significant; in the Wilcoxon test, considering that the results for both samples resulted in a level of significance lower than  $\alpha = 0.05$ ; it can be concluded that the height distributions of invasive species are different between the two sample areas studied. This can be easily seen in Figures 5 and 7, where it is possible to notice that there is a visual difference in the height distribution of invasive species in the two models analyzed for both sample areas, and this phenomenon is due to the accuracy of the compared models. It can be seen in Figure 9 the presence of invasive species for both

sample areas, where the points of height measurements of *Urochloa spp.* found at the site were collected, the collection points being photographed.

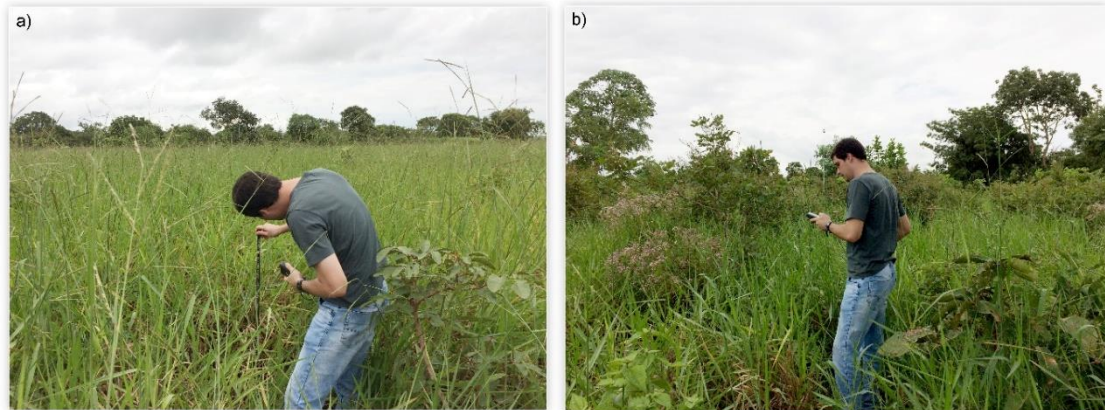


Figure 9 - In (a) amostal area 1 with the presence of *Urochloa spp.* In (b) sample area 2 with the presence of *Urochloa spp.* mixed with vegetation fragments. Source: The authors.

#### 4. DISCUSSION

Regarding the objective of this research -- analyzing the accuracy of the CHIS+GNSS(I) model of an invasive species canopy altitude pattern and its distribution -- a different behavior was verified in the two test sample areas. In sample area 1, the canopy height variation of exotic grasses was reduced in both models. The main reason for this is probably that the sample area 1 presents a more homogeneous topography than the sample area 2. Furthermore, it was observed in the field the presence of invasive species in both sample areas, which showed presence of invasive species in the reference model (CHIS+GNSS(RTK)), and in some parts of sample area 1 and most evidently of sample area 2 there was no invasive species in the estimated model (CHIS+GNSS(I)).

The accuracy error of the model on XYZ axes is smaller when using the CHIS+GNSS(RTK) model. Sample area 2 showed a different pattern in the accuracy of the CHIS+GNSS(I) model on component Z (height) probably due to the natural differences in terrain elevation.

The CHIS+GNSS(I) method is less accurate than the CHIS+GNSS(RTK) model, showing a systematic shift due to the combined error sources of the XYZ axes shift, aligned with the lack of any background reference point (RTK).

The CHIS+GNSS(I) model with the maximum difference observed in the mean error test (RMSE<sub>z</sub>) was 24 cm, this is unsuitable for works that require greater positional accuracy, such as precision agriculture.

Economic cost, time invested and requirements of each model are different and can serve various remote sensing purposes. It is noteworthy that even if field operation uses only GNSS, it can thus be resampled to a grosser simple pixel size to absorb the geometric uncertainty, which is typically the radial error, i.e. this would allow the use of the model for analysis on a grosser

analysis scale, for example, to determine average canopy height variations in hectares but not square meters.

From all these findings, it was possible to extract some important results to actually use the CHIS+GNSS(I) model. First of all, if the terrain it is no so rippled, the CHIS+GNSS(I) model becomes viable, at least in part, such as when the canopy survey does not require minimum heights like those used in this study. The inclusion of RTK-based image position observations in the UAV processing workflow turned out to have a positive effect, particularly on the height component.

In the future, all UAVs in the market are expected to be equipped with hardware for UAV image tagging (geolocation) that can correct aerial photo positioning errors in a centimeter scale (TOMASTIK *et al.*, 2019). Areas such as Restoration Ecology and Ecological Restoration are also expected to incorporate multitemporal data with high spatial and temporal resolution, and positional accuracy for monitoring vegetation in recovery in their research and work routines. However, even with distortions of positional data, these activities still have access to robust data for studies on degraded ecosystems (PÁDRO *et al.*, 2019).

In some areas, such as agriculture, surveying the weeds canopy, which is very common in agriculture, from the UAV may not be possible because the size of this vegetation type is very small and the precise georeferencing is indispensable (BIRDAL *et al.*, 2017; VETRELLA *et al.*, 2018). A suggestion for improving survey accuracy, such as that of this study, would include the integration of an RTK-GPS device such as the Trimble BD 935 into a rotary wing platform potentially mounted directly to the gimbal, or even the camera. If it were also possible to approximate the altitude of the optical axis, in addition to a precise position, at least a faster and more efficient camera orientation can be expected. Alsadik *et al.* (2013) have already shown that knowledge of approximate camera locations and

viewing direction can decrease processing time tremendously while increasing overall reliability (GERKE *et al.*, 2016).

## 5. FINAL CONSIDERATIONS

In this work we tested the accuracy of the CHIS+GNSS(I) model and demonstrated that the spatial height (z) data were relatively accurate when compared to data obtained using standard reference approaches (CHIS+GNSS(RTK)). Additional factors may have a supposedly significant influence on accuracy, such as terrain altitude differences. More specifically, this study investigated the impact of invasive species surveys without the conventional RTK control station. Results from RTK are more accurate and less inclined to error.

When the approach is to carry out a plant height survey in the range of centimeters, e.g. weeds in agriculture, it is recommended that the survey be from RTK. The technique of canopy height survey is interesting to measure indicators of recovery of vegetated areas and degraded and altered areas recomposition projects. Increasing the number of ground control points (GCPs) would likely lead to increases in accuracy, but such an approach is most feasible when the job requirement is of minimum accuracy, however, only the use of RTK does not guarantee accuracy. In the two sample areas, the horizontal RMSEs and MAEs (z) of the CHIS+GNSS(I) method did not exceed 30 cm, showing relative accuracy. The results suggest that the CHIS+GNSS(I) method can provide data with satisfactory accuracy compared to GCP approaches, regardless of terrestrial measurements, for applications that do not require centimeter positional accuracy.

This model can be strategic for the remote detection of inaccessible and dangerous forest areas that do not require high spatial accuracy, allowing the measurement of canopy variation and presence of clearings, that is, ecological aspects of the ecosystem. If the main question was whether the CHIS+GNSS(I) model could be the best solution in terms of economics, flexibility and time to map hard-to-reach areas that do not require high accuracy, the answer could be: yes. However, besides additional accuracy ambiguity testing, also the UAV technical parameters (maximum flight time, unattended operation, etc.) must be adjusted to fully benefit from these possibilities.

The method analyzed here can be useful when preparing inventories for areas with degraded native vegetation, which are usually done manually and ocularly by man, and is also a means of monitoring them at defined intervals to identify the presence of species that inhibit the development and growth of areas in environmental recovery. UAV technology is highly cost effective, flexible and mobile, in addition to fully automated photogrammetric processing, it can be deployed at very low cost for operational use.

## 6. REFERENCES

ALSADIK, B.; GERKE, M.; VOSSSELMAN, G. Automated camera network design for 3D modeling of cultural heritage objects. *Journal of Cultural Heritage*, v. 14, 515-526, 2013.

AGISOFT PHOTOSCAN PROFESSIONAL (Version 1.4.0) (Software). 2017. Retrieved from <http://www.agisoft.com/downloads/installer/>

AUGUIE, B. 2017. gridExtra: Miscellaneous Functions for "Grid" Graphics. R package version 2.3. <https://CRAN.R-project.org/package=gridExtra>

AKOGLU, H. User's guide to correlation coefficients. *Turkish Journal of Emergency Medicine*, v. 18, 91-93, 2018.

BIVAND, R.; KEITT, T.; ROWLINGSON, B. 2018. rgdal: Bindings for the 'Geospatial' Data Abstraction Library. R package version 1.3-4. <https://CRAN.R-project.org/package=rgdal>

CHRISTIE, K. S.; GILBERT, S. L.; BROWN, C. L.; HATFIELD, M.; HANSON, L. Unmanned aircraft systems in wildlife research: Current and future applications of a transformative technology. *Front. Ecol. Environ.*, v. 14, 241-251, 2016.

CHABOT, D.; BIRD, D. M. Wildlife research and management methods in the 21st century: Where do unmanned aircraft fit in? *J. Unmanned Veh. Syst.*, v. 3, 137-155, 2015.

CHAI, T.; KIM, H. C.; LEE, P.; TONG, D.; PAN, L.; TANG, Y.; HUANG, J.; MCQUEEN, J.; TSIDULKO, M.; STAJNER, I. Evaluation of the United States National Air Quality Forecast Capability experimental real-time predictions in 2010 using Air Quality System ozone and NO<sub>2</sub> measurements. *Geosci. Model Dev.*, v. 6, 1831-1850, 2013.

CHAI, T.; DRAXLER, R. R. Root mean square error (RMSE) or mean absolute error (MAE)? – Arguments against avoiding RMSE in the literature. *Geosci. Model Dev.*, v. 7, 1247-1250, 2014.

DVORÁK, P.; MULLEROVÁ, J.; BARTALOS, T.; BRUNA, J. Unmanned Aerial Vehicles For Alien Plant Species Detection And Monitoring. In: *INTERNATIONAL CONFERENCE ON UNMANNED AERIAL VEHICLES IN GEOMATICS*, Toronto: Canada, 83-90, 2015.

DE SÁ, N. C.; CASTRO, P.; CARVALHO, S.; MARCHANTE, E.; LÁPEZ-NÚÑEZ, F. A.; MARCHANTE, H. Mapping the Flowering of an Invasive Plant Using Unmanned Aerial Vehicles: Is There Potential for Biocontrol Monitoring?. *Frontiers in Plant Science*, v. 9, 283, 2018.

DEEPAYAN, S. 2008. Lattice: Multivariate Data Visualization with R. Springer, New York. ISBN 978-0-387-75968-5.

EMPRESA BRASILEIRA DE PESQUISA AGROPECUÁRIA- EMBRAPA. *Sistema brasileiro de classificação de solos*. 3ª. ed. Rio de Janeiro: EMBRAPA-SPI, 2006. 306 p.

FOWLER, J.; COHEN, L.; JARDIS, P. Practical Statistics for Field Biology. 2. ed., Loughborough: Wiley, 2009. 132p.

FORTES, E. P. Seed Plant Drone for Reforestation. *The Graduate Review*, v. 2, 13-26, 2017.

- GERKE, M.; PRZYBILLA, H. J. Accuracy Analysis of Photogrammetric UAV Image Blocks: Influence of Onboard RTK-GNSS and Cross Flight Patterns. *Photogrammetrie – Fernerkundung – Geoinformation*, v. 1, 17-30, 2016.
- GONÇALVES, J.; HENRIQUES, R.; ALVES, P.; SOUSA-SILVA, R.; MONTEIRO, A. T.; LOMBA, Â.; MARCOS, B.; HONRADO, J. Evaluating an unmanned aerial vehicle-based approach for assessing habitat extent and condition in fine-scale early successional mountain mosaics. *Appl. Veg. Sci.*, v. 19, 132-146, 2016.
- GOOGLE. Google Earth website. <http://earth.google.com/>, Data da imagem: 26/02/2019.
- HAUKE, J.; KOSSOWSKI, T. Comparison of values of Pearson's and Spearman's correlation coefficients on the same sets of data. *Quaestiones Geographicae*, v. 30, 87-93, 2011.
- HIJMANS, R. J. 2017. raster: Geographic Data Analysis and Modeling. R package version 2.6-7. <https://CRAN.R-project.org/package=raster>.
- HUNG, C.; XU, Z. SUKKARIEH, S. Feature Learning Based Approach for Weed Classification Using High-Resolution Aerial Images from a Digital Cameral Mounted on a UAV. *Remote Sensing*, v. 6, 12037–12054, 2014.
- INSTITUTO BRASILEIRO DE GEOGRAFIA E ESTATÍSTICA (IBGE). Disponível em: <https://www.ibge.gov.br/geociencias/downloads-geociencias.html>. Acessado em: 12/01/2019.
- JUFFE-BIGNOLI, D.; BURGESS, N. D.; BINGHAM, H.; BELLE, E. M. S.; DE LIMA, M. G.; DEGUIGNET, M.; BERTZKY, B.; MILAM, N.; MARTINEZ-LOPEZ, J.; LEWIS, E.; EASSOM, A.; WICANDER, S.; GELDMANN, J.; VAN SOESBERGEN, A.; ARNELL, A. P.; O'CONNOR, B.; PARK, S.; SHI, Y. N.; DANKS, F. S.; MACSHARRY, B.; KINGSTON, N. Protected Planet Report 2014. UNEP-WCMC: Cambridge, UK, 2014. 69 p.
- KLOBE, J.; MCKEAN, J. W. Nonparametric Statistical Methods Using R. 1. ed. Flórida: CRC Press, 2014. 287p.
- KRULL, W.; TOBERA, R.; WILLMS, I.; ESSEN, H.; WAHL, N. V. International Symposium on Safety Science and Technology Early forest fire detection and verification using optical smoke, gas and microwave sensors. *Procedia Engineering*, v. 45, 584-594, 2012.
- KOH, L. P.; WIH, S. A. Dawn of drone ecology: low-cost autonomous aerial vehicles for conservation. *Tropical Conservation Science*, v. 5, 121-132, 2012.
- KNOTH, C.; KLEIN, B.; PRINZA, T.; KLEINBECKER, T. Unmanned Aerial Vehicles as Innovative Remote Sensing Platforms for High-Resolution Infrared Imagery to Support Restoration Monitoring in Cut-Over Bogs. *Applied Vegetation Science*, v. 16, 509-517, 2013.
- LAMIGUEIRO, O. P.; HIJMANS, R. 2018. rasterVis. R package version 0.45.
- LINCHAT, J.; LISEIN, J.; SEMEKI, J.; LEJEUNE, P.; Vermeulen, C. Are unmanned aircraft systems (UASs) the future of wildlife monitoring? A review of accomplishments and challenges. *Mamm. Rev.*, v. 45, 239-252, 2015.
- LOPOUKHINE, N.; CRAWHALL, N.; DUDLEY, N; FIGGIS, P.; KARIBUHOYE, C.; LAFFOLEY, D.; LONDOÑO, J. M.; MACKINNON, K.; SANDWITH, T. Protected areas: providing natural solutions to 21st Century challenges. *Surveys and Perspectives Integrating Environment and Society*, v. 5, 1-16, 2012.
- LÓPEZ, J. J.; MULERO-PÁZMÁNY, M. Drones for Conservation in Protected Areas: Present and Future. *Drones*, v. 3, 10, 2019.
- MATESE, A.; GENNARO, S. F. D.; BERTON, A. Assessment of a canopy height model (CHM) in a vineyard using UAV-based multispectral imaging. *INTERNATIONAL JOURNAL OF REMOTE SENSING*, v. 38, 2150-2160, 2017.
- MCKEEN, S. A.; WILCZAK, J.; GRELL, G.; DJALALOVA, I.; PECKHAM, S.; HSIE, E.; GONG, W.; BOUCHET, V.; MENARD, S.; MOFFET, R.; MCHENRY, J.; MCQUEEN, J.; TANG, Y.; CARMICHAEL, G. R.; PAGOWSKI, M.; CHAN, A.; DYE, T.; FROST, G.; LEE, P.; MATHUR, R. Assessment of an ensemble of seven realtime ozone forecasts over eastern North America during the summer of 2004. *J. Geophys. Res.*, v. 110, D21307, 2005.
- MICHEZ, A.; PIÉGAY, H.; JONATHAN, L.; Claessens, H.; Lejeune, P. Mapping of Riparian Invasive Species with Supervised Classification of Unmanned Aerial System (UAS) Imagery. *International Journal of Applied Earth Observation and Geoinformation*, v. 44, 88-94, 2016.
- MARTIN, F.; MULLERONÁ, J.; BORGNIET, L.; DOMMANGET, F.; BRETON, V.; EVETTE, A. 2018. Using Single- and Multi-Date UAV and Satellite Imagery to Accurately Monitor Invasive Knotweed Species. *Remote Sens.*, v. 10, 1662.
- MULERO-PÁZMÁNY, M.; STOLPER, R.; VAN ESSEN, L. D.; NEGRO, J. J.; SASSEN, T. Remotely piloted aircraft systems as a rhinoceros anti-poaching tool in Africa. *PLoS One*, v. 9, 1-10, 2014.
- MERINO, L.; CABALLERO, F.; MARTÍNEZ-DE-DIOS, J. R.; MAZA, I.; OLLERO, A. An Unmanned Aircraft System for Automatic Forest Fire Monitoring and Measurement. *J Intell Robot Syst.*, v. 65, 533-548, 2012.
- MELESSE, A.; Weng, Q.; Prasad, S. Senay, G. Remote Sensing Sensors and applications in environmental resources mapping and modelling. *Sensors*, v. 7, 3209-3241, 2007.

- NEUWIRTH, E.; 2014. RColorBrewer: ColorBrewer Palettes. R package version 1.1-2. <https://CRAN.R-project.org/package=RColorBrewer>
- PADRÓ, J. C.; MUÑOZ, F. J.; PLANAS, J.; PONS, X. Comparison of four UAV georeferencing methods for environmental monitoring purposes focusing on the combined use with airborne and satellite remote sensing platforms. *Int J Appl Earth Obs Geoinformation*, v. 75, 130–140, 2019.
- PEEL, M. C.; FINLAYSON, B. L. MCMAHON, T. A. Updated world map of the Köppen-Geiger climate classification. *Hydrol. Earth Syst. Sci.*, v. 11, 1633–1644, 2007.
- PEÑA, J. M.; TORRES-SÁNCHEZ, J.; DE CASTRO, A. I.; KELLY, M.; LÓPEZ-GRANADOS, F. Weed Mapping in Early-Season Maize Fields Using Object-Based Analysis of Unmanned Aerial Vehicle (UAV) Images. *PlosOne*, v. 8, e77151, 2013.
- RODRÍGUEZ, A.; NEGRO, J. J.; MULERO, M.; RODRÍGUEZ, C.; HERNÁNDEZ-PLIEGO, J.; BUSTAMANTE, J. The Eye in the Sky: Combined Use of Unmanned Aerial Systems and GPS Data Loggers for Ecological Research and Conservation of Small Birds. *PLoS One*, v. 7, 1-6, 2012.
- R CORE TEAM. 2019. R: A language and environment for statistical computing. R Foundation for Statistical Computing, Vienna, Austria. URL: <https://www.R-project.org/>.
- SAVAGE, N. H.; AGNEW, P.; DAVIS, L. S.; ORDÓÑEZ, C.; Thorpe, R.; Johnson, C. E.; O'Connor, F. M.; Dalvi, M. Air quality modelling using the Met Office Unified Model (AQUM OS24-26): model description and initial evaluation. *Geosci. Model Dev.*, v. 6, 353-372, 2013.
- SOUZA, A. P.; MOTA, L. L.; ZAMADEI, T.; MARTIM, C. C.; ALMEIDA, F. T.; PAULINO, J. Classificação climática e balanço hídrico climatológico no Estado de Mato Grosso. *Nativa*, v. 1, 34-43, 2013.
- STROPPIANA, D.; VILLA, P.; SONA, G.; RONCHETTI, G.; CANDIANI, G.; PEPE, M.; Busetto, L.; MIGLIAZZI, M.; BOSCHETTI, M. Early season weed mapping in rice crops using multi-spectral UAV data. *INTERNATIONAL JOURNAL OF REMOTE SENSING*, v. 39, 5432-5452, 2018.
- VILJANEN, N.; HONKAVAARA, E.; NASI, R.; HAKALA, T.; NIEMELAINEN, O.; KAIVOSOJA, J. A Novel Machine Learning Method for Estimating Biomass of Grass Swards Using a Photogrammetric Canopy Height Model, Images and Vegetation Indices Captured by a Drone. *Agriculture*, v. 8, 70, 2018.
- WATSON, J. E. M.; DUDLEY, N.; SEGAN, D. B. HOCKINGS, M. The performance and potential of protected areas. *Nature*, v. 515, 67–73, 2014.
- WAN, H.; WANG, Q.; JIANG, D.; FU, J.; YANG, Y.; LIU, X. Monitoring the Invasion of *Spartina Alterniflora* Using Very High Resolution Unmanned Aerial Vehicle Imagery in Beihai, Guangxi (China). *The Scientific World Journal*, v. 2014, 1–7, 2014.
- WHITEHEAD, K.; HUGENHOLTZ, C. H. Remote sensing of the environment with small unmanned aircraft systems (UASs), part 1: A review of progress and challenges. *J. Unmanned Veh. Syst.*, v. 2, 69-85, 2014.
- ZAMAN, B.; JENSEN, A. M.; MCKEE, M. Use of High-Resolution Multi-Spectral Imagery Acquired with an Autonomous Unmanned Aerial Vehicle to Quantify the Spread of an Invasive Wetlands Species. In: *GEOSCIENCE AND REMOTE SENSING SYMPOSIUM (IGARSS)*, Vancouver: BC, Canada, 803-806, 2011.
- ZILIANI, M. G.; PARKES, S. D.; HOTEIT, I.; MCCABE, M F. Intra-Season Crop Height Variability at Commercial Farm Scales Using a Fixed-Wing UAV. *Remote Sens.*, v. 10, 2007, 2018.
- ZHANG, Q.; QIN, R.; HUANG, X.; FANG, Y.; LIU, L. Classification of ultra-high resolution orthophotos combined with DSM using a dual morphological top hat profile. *Remote Sens.*, v. 7, 16422-6440, 2015.

## 7. ACKNOWLEDGEMENT

The authors would like to express their gratitude to the Graduate Program in Environmental Management and Technology (PGTA), at the Federal University of Rondonópolis (UFR).

This study was carried out with the support of the Federal University of Rondonópolis – UFR/MEC – Brazil.

The research was also made possible by the Coordenação de Aperfeiçoamento de Pessoal de Nível Superior (CAPES), Brazil, for the financial support needed to carry out this research. Financing Code 001 and Conselho Nacional de Desenvolvimento Científico e Tecnológico (CNPq) (Processes 441975/2018-6, 305013/2018-1 and 315170/2018-2).

Moreover, we would like to thank the CNPq (National Council for Scientific and Technological Development) for the research productivity grant provided to A. C. Paranhos Filho (CNPq Process 305013/2018-1).

We are grateful to CAPES for providing us with access to the Journal Portal.

Finally, we would also like to thank CAPES for Dhonatan Diego Pessi's master scholarship and doctoral scholarship (case number 88887.494036/2020-00).

Received in: 16/04/2020

Accepted for publication in: 29/08/2021